DOI: 10.13009/EUCASS2023-904
Aerospace Europe Conference 2023 – 10TH EUCASS – 9TH CEAS

Environmental and Economic Assessment of Alternative Fuels and Powertrains on Aircraft Level

Felix Brenner† Jonas Mangold* Dominik Eisenhut* Andreas Strohmayer**
** University of Stuttgart*
Pfaffenwaldring 31, 70569 Stuttgart, Germany
brenner@ifb.uni-stuttgart.de– mangold@ifb.uni-stuttgart.de– eisenhut@ifb.uni-stuttgart.de
– strohmayer@ifb.uni-stuttgart.de
† Corresponding Author

Abstract
In the frame of the H2020 project FUTPRINT50 a 50-passenger, 400 km-range hybrid-electric aircraft was designed for entry into service by 2035. In this paper, three internal combustion engine (ICE) aircraft – powered by Sustainable Aviation Fuel, hydrogen and methane – and a hybrid-electric aircraft, featuring gas turbine and electric motors are analysed using the SUAVE framework and compared to the hybrid-electric variant. Results show, that the hybrid-electric configuration bears high operating costs due to the mass of its electric components. Finally, looking at the different fuels it becomes apparent, that hydrogen is the only option where a renewable production path leads to a higher figure of merit.

1. Introduction

Reducing the climate impact of aviation is a pressing topic of today's research. In the scope of FUTPRINT50, hybrid-electric aircraft with an anticipated entry into service (EIS) by 2035 are investigated. Within the project, different propulsion architectures have shown promising results regarding the reduction of climate impact. However, all improvements are highly dependent on the improvement of current battery technologies. With regards to these uncertainties it is necessary to also focus on other climate friendly alternatives. For this paper, three technologies are compared to the reference hybrid-electric aircraft designed for FUTPRINT50 and to the ATR 42-500 as todays reference [1]. These three aircraft are powered by improved gas turbines (year 2035 technologies), the main emission reduction however is achieved by using alternative fuels.

A first aircraft design is fuelled with Sustainable Aviation Fuel (SAF) and is also used as the conventional reference aircraft (CRA 2040) in FUTPRINT50. Besides being capable of using 100 % SAF, the aircraft based on an ATR 42-500 also features a higher aspect ratio wing, improved structural materials, e.g. carbon fiber reinforced polymers (CFRP) for the wings, fuselage and empennage, as well as more efficient engines. Furthermore, the CRA 2040 is capable of carrying a heavier payload (5300 kg) over the same design range (1555 km) as the ATR predecessor. The final configuration of the CRA 2040 is shown in Figure 1.

Figure 1: FUTPRINT50 conventional reference aircraft (CRA 2040)

DOI: 10.13009/EUCASS2023-904

The second aircraft investigated for this study is fuelled by liquid hydrogen (LH2). In the following, this aircraft will be referred to as hydrogen reference aircraft (HRA). This aircraft is designed to the same top-level aircraft requirements (TLARs) as the CRA 2040. The large insulated storage tanks anticipated for liquid hydrogen need to be installed within the HRAs fuselage [2]. This results in a longer fuselage with more drag, heavier wings and an increased empty mass compared to the CRA 2040.

Similar assumptions apply for the third aircraft, a turboprop fuelled with liquefied methane/natural gas (LNG). In the following, this aircraft will be referred to as the methane reference aircraft (MRA). The higher volumetric energy density of LNG results in a smaller fuel tank and thus a shorter fuselage with less drag compared to the HRA. All aircraft are implemented in the SUAVE framework and compared based on emissions and fuel costs (both for fossil and renewable energy sources).

In Section 2, this paper initially presents the requisite background for obtaining the properties and characteristics of the investigated fuels. Subsequently, Section 3 describes the methodology for designing the corresponding aircraft configurations, the implications of utilizing cryogenic fuels, and the assessment method. A case study is conducted in Section 4 to evaluate meaningful and competitive payload range capabilities. The environmental and economic assessment of the resulting aircraft designs is presented in Section 5. Lastly, Section 6 showcases the obtained results and offers an outlook for future research activities.

2. Fuel characteristics

The three fuels main characteristics regarding energy density and storage condition are given in Table 1. These values are assumed for liquid state storage at 1 bar. For cryogenic fuels, LNG and LH2, the density is used in a thermodynamically saturated state (saturated liquid) [2]. In addition to the storage requirements, the gravimetric index (GI) of the fuel tank is listed in the table. The GI is defined as in equation (1).

$$GI = \frac{m_{\text{Fuel}}}{m_{\text{Tank}} + m_{\text{Fuel}}} \tag{1}$$

Considering the system-specific energy (GI combined with gravimetric energy density), as introduced in Mangold et al. [2], all three fuels have the same system-specific energy with approximately 43 MJ/kg. Thus, the evaluation in Section 4 is almost independent of the gravimetry energy density. In other words, advantages or disadvantages through the gravimetric energy density are basically negligible.

Table 1: Characteristics of the investigated fuel types [3, 4]

	Jet A-1/SAF	**LNG**	**LH2**
Gravimetric energy density in MJ/kg	43.0	55.0	120.0
Density in kg/m^3	800	450	70.8
Liquid state temperature in K	226.15 to 566.15	91.48 to 111.15	14.01 to 20.35
Fuel tank gravimetric index GI	N/A	0.8	0.35

The three fuels SAF, LH2 and LNG all promise a reduction in lifecycle CO2 emissions. However, the net CO2 emissions of the fuel heavily depend on the production method. The fuel prices as listed in Table 2 are hard to estimate since they cover a large range and future demands are just extrapolations. LNG can be differentiated between fossil sourced LNG and LNG from renewable sources such as biogas. In this study, the fuel price is assumed to be directly linked to the net carbon intensity. To that end, the lowest price is associated to fossil LNG with a price of 0.4 \$/kg or 0.0073 \$/MJ and carbon neutral bio-LNG with a maximum price of 2.4 \$/kg or 0.0438 \$/MJ; these are current numbers that may change in future scenarios. Liquid hydrogen is assumed to be produced either green or grey with a net carbon intensity between 0 and 10.6 kg_{CO2}/kg_{LH2} [5]. Just as for LNG, it is assumed that the price increases linearly from fossil sourced to completely renewably sourced LH2, with a price range of 1 \$ to 5 \$ per kg or 0.0083 \$/MJ to 0.0416 \$/MJ.

DOI: 10.13009/EUCASS2023-904

The price range for conventional jet fuel is similar to that of liquid hydrogen when comparing prices on a $/kg basis, ranging from 1 $/kg for fossil Jet A-1 to 5 $/kg for carbon neutral SAF. Since the gravimetric energy density of kerosene is lower than that of LH2 however, the price in $/MJ is significantly higher for Jet A-1 and SAF with prices between 0.0233 $/MJ and 0.1163 $/MJ.

Table 2: Fuel cost comparison between Jet A-1/SAF, LNG and LH2 based on 2023 values [6, 7, 8, 9, 10, 11, 12]

	Jet A-1/SAF	**LNG**	**LH2**
Minimum Price in $/kg	1	0.4	1
Minimum Price in $/MJ	0.0233	0.0073	0.0083
Maximum Price in $/kg	5	2.4	5
Maximum Price in $/MJ	0.1163	0.0438	0.0416

As can be seen in Table 2, the fuel price of LNG seems the lowest, both fossil and renewably sourced, when referring to $/kg. However, since all fuels have different gravimetric energy densities, the comparison is not conclusive. Hence, for this investigation, the prices are compared on a $/MJ basis. This comparison shows, that LNG and LH2 produced from fossil sources or using fossil energy are the most cost-efficient fuels as of today. Both fuels are less than half the price of fossil Jet A-1. The price range of LNG and LH2 when compared at this basis is similar, while there is a large gap to Jet A-1 and SAF. Figure 2 shows the relation of fuel cost in $/MJ to the net carbon intensity of the fuel. The net emissions of methane range from 0 kg CO2 per kg LNG for renewably sourced LNG to 2.75 kg CO2 per kg LNG for fossil methane. While grey hydrogen has a very high carbon intensity of 10.6 kg CO2 per kg LH2, the gradient to green hydrogen is rather steep. This results in LH2 having the lowest price per MJ for a net zero fuel, closely followed by bio-LNG. Jet A-1 does have a cost advantage over LH2 for carbon intensities between 3.16 kg CO2 per kg fuel to 2.85 kg CO2 per kg fuel. However, it falls behind of LNG in every point. This shows that there is no cost advantage in using SAF compared to the other alternatives, when neglecting aircraft development and infrastructure costs.

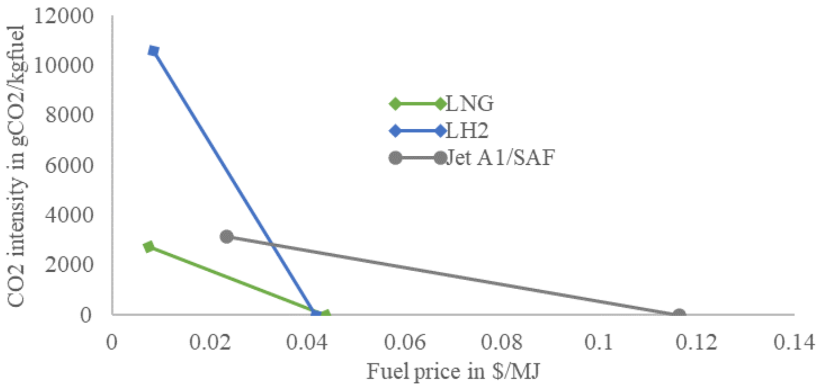

Figure 2: Assumed fuel pricing scenario for low lifecycle CO2

Besides CO2, NOx emissions are identified as a main contributor to aviation induced global warming [13]. It's relative impact increases for aircraft flying at altitudes at which no contrails are produced. It is assumed, that both methane and hydrogen combustion will have a positive impact on the NOx emissions. The emission indexes (EI) assumed for the calculations in this study are listed in Table 3.

Table 3: Emission indexes of each fuel (Tail pipe only)

	Jet A-1/SAF	**LNG**	**LH2**
CO2 in kg_{CO2}/kg_{fuel}	3.16	2.75	0
NOx in %	100	75	76

DOI: 10.13009/EUCASS2023-904

The NOx EI of LNG is 25 % lower compared to Jet A-1 [14] and that of LH2 is 24 % lower on a $kg_{pollutant}/kg_{fuel}$ basis [15]. The NOx values do not change from fossil to renewable fuels. The CO2 EI given above are tailpipe emissions only and are equal for fossil and renewable fuels. Typically, SAF can only reduce lifecycle CO2 emissions by a maximum of 80 % [16], a reduction of 100 % is assumed in this study only for a better comparability of the different fuels.

3. Overall aircraft design methodology

This chapter presents the methodology for calculating and designing the effects of different fuels on powertrain architectures. First, the propulsion architectures are introduced to determine the influence of the fuel on the overall aircraft design. The utilization of cryogenic fuels necessitates an additional tank. Subsequently, the adaptations required for the iterative aircraft design process are elaborated upon, as they are essential for achieving a converged aircraft. These adaptations primarily involve modifying the engine and integrating the tank. To assess the resulting designs, the evaluation criteria are explained. To ensure a consistent basis for comparison, the evaluation is conducted based on the same mission definition.

3.1 Powertrain architectures

The investigated powertrain architectures are shown in Figure 3. The ATR 42-500, the CRA as well as the HRA and MRA use a conventional layout with two turboprops, one attached on each wing. The HEA additionally has two wingtip propellers which are solely powered by electric motors. Furthermore, the gas turbines can be either boosted by the electric motor or they are used as generators to either recharge the battery or power the wingtip propellers.

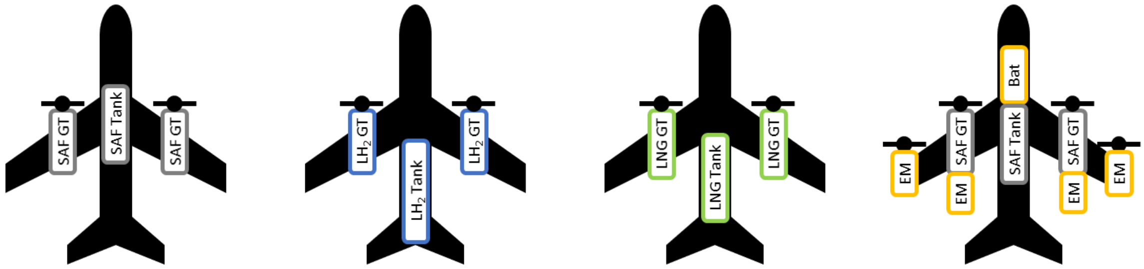

Figure 3: Investigated powertrain architectures, from left to right: CRA (ATR 42-500), HRA, MRA, HEA; adapted from Affonso et al. [17]

The tanks for the Jet A1/SAF aircraft are located in the wings. For the HRA and MRA, the tanks are located in the aft section of the fuselage.

3.2 Aircraft design in SUAVE

The respective aircraft designs are based on advancements on the open-source tool SUAVE [18]. SUAVE, originally developed by Stanford University [19], is a preliminary aircraft design environment, which allows for the implementation of new methods. Therefore, during the FUTPRINT50 project, several different propulsion architectures and aircraft configurations were developed and implemented in a GitHub Fork [20].

The conventional aircraft, i.e. the ATR 42-500 and the CRA 2040, both are designed with the constrains described in the introduction [21]. For the HEA, a detailed case study was performed to find a reasonable parameter setup for a competitive aircraft [22]. Thus, the methodology and enhancements for cryogenic fuels for the HRA and MRA are described in the following section. The adaptions are mainly the changed fuselage due to the tank and the engine scaling due to the different specific energies of the fuels. For the cryogenic fuels, which cannot be efficiently stored in the wings, an additional tank is needed. There are several options for its location, in this study it is placed in the rear fuselage behind the pressure bulkhead. However, the cabin, in particular its length, remains unchanged, which means that the aircraft fuselage becomes longer due to the cryogenic fuel tank behind the rear pressure bulkhead. The tank has a cylindric shape (preferably Kloepper-type shape).

DOI: 10.13009/EUCASS2023-904

The additional fuselage length $\Delta l_{fuselage,tank}$ is based on the fuel volume $V_{fuel,design\ point}$, allowances a, the fuselage diameter $d_{fuselage}$ and an additional diameter factor $f_{diameter}$:

$$\Delta l_{fuselage,tank} = V_{fuel,design\ point} / \left(a \cdot \pi \cdot \left(f_{diameter} \cdot d_{fuselage} \right)^2 \right) \quad \mathbf{(2)}$$

The $V_{fuel,design\ point}$ is calculated for the required fuel mass of the design mission (see Section 4) and the corresponding fuel density, see Table 1. The allowances account for non-useable volume of the tank and are estimated with 7.3% [23]. The thermodynamic behaviour during the mission is not considered. The diameter factor is related to the tank diameter and length. It sets the length to diameter ratio of the tank to a reasonable value, in order to not create a very short cylinder with a large diameter. Additionally, this factor accounts for insulation and relates to the outer diameter of the tank.

Through the GI, (see equation 1), the empty mass of the fuel tank can be determined with the design mission fuel mass. In comparison to conventional aircraft, this relation affects the payload range diagram, see Section 4. This additional mass is added to the mass breakdown of the aircraft and effects the Operating Empty Mass (OEM). Through an iterative sizing loop, snowball effects are considered until the sizing converges. Additionally, the cryogenic fuel tank in the rear fuselage affects the center of gravity (CG) of the aircraft. To ensure sufficient static stability of each aircraft design evaluated in SUAVE, the sizing process is directly coupled with integrated stability analyses. In each iteration step, the center of gravity is calculated based on the mass and position of every single component (including fuel tank), determining the position of the main wing under the assumption of a fixed center of gravity relative to the main wing's mean aerodynamic chord (MAC). The vertical and horizontal stabilizers are then sized based on a fixed value for their volume coefficient and their position, which is determined by the sizing of the fuselage. The center of gravity, main wing position, and empennage surface areas are adjusted during the iteration process until convergence is achieved. Therefore, all aircraft designs have similar center of gravities related to the MAC.

The turboprop engine is modelled with an engine deck surrogate [21]. It is influenced by the altitude, Mach number and throttle and interpolates the required return values, such as actual power, fuel mass flow and the inputs for the emissions model. To transfer the conventional Jet A-1 combustion engine for cryogenic fuels, a scaling of the specific fuel consumption (SFC) is implemented. That scaling relates to the specific energy of the respective fuel (see Table 1), which means that all engines have the same specific energy consumption and therefore the same efficiency. Mangold et al. already showed that the combustion of different fuels has similar thermal efficiencies [24] and thus, this is assumed for the investigation in this study.

For assessing and comparing the resulting aircraft, CRA, HEA, MRA and HRA, Figures of Merit (FOM) are used [18, 24]. This methodology is advantageous for comparing different evaluation criteria, that are difficult to combine. After scaling and weighting, this results in one single number, which shows the overall performance obtained with this method. The FOM are influenced by environmental and technical challenges, as well as the cash operating costs (COC), see Figure 4.

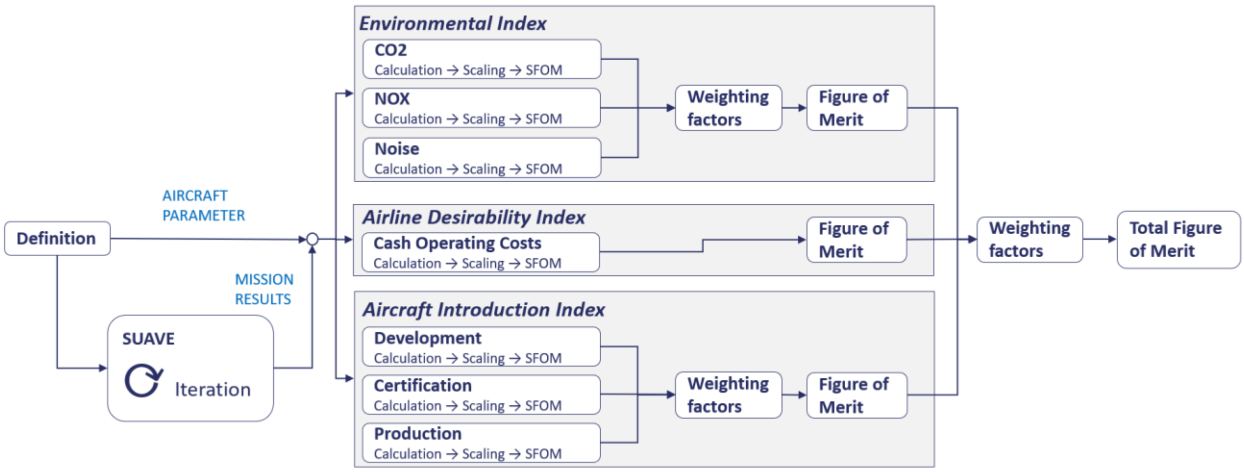

Figure 4: Calculation process of Figures of Merit [18]

DOI: 10.13009/EUCASS2023-904

The environmental index describes the environmental impact of the aircraft. It includes CO2, NOx and noise emissions. CO2 is calculated using the linear relationship of CO2 emitted per 1 kg of fuel burned [25]. To account for different CO2 intensities, a factor is applied to described the behavior of Table 3. NOx emissions are calculated using the P3T3 method [21] in combination with adopted emission indices in Table 3. The Global Warming Potential (GWP) model by Svensson [26] is applied to account for different flight altitudes and the effects to the atmosphere. The COCs are determined using the method from Thorbeck [27], adjusted for hybrid-electric aircraft by Hoelzen et al. [12]. Additional information about usability, methodology and calculation can be found in Mangold et al. [18]. In the COCs, the fuel prices of Table 2 are included.

For the performance comparison in Chapter 4, there are four different FOMs: FOM_total consist of the COCs and the environmental index. For the FOM_environmental, also production and development costs as well as certification risks are included. The FOM_COC covers the COCs and FOM_CO2 describes CO2 emissions. The scaling of the FOMs relate to the reference aircraft (ATR 42-500), which is determined for an off-design mission with 5300 kg payload and a range of 400 km as described in Section 3.3. This practical scaling allows easy comparison with the targets set in Flightpath 2050 [28] and the Green Deal [29]. The reference aircraft's (ATR 42-500) FOM is set to 0. A FOM of +1 is 100 % better as the reference and a FOM of -1 is 100 % worse respectively.

3.3 Mission description for assessment and evaluation

The evaluation mission for all aircraft investigated is based on the reference mission for hybrid electric regional aircraft as defined in FUTPRINT50. The 400 km mission is carried out with a payload of 5300 kg, which covers 80 % of world-wide regional air travel [30]. Through the analysis of the same off-design mission, the assessment is meaningfully comparable. As described in Section 3.2, the FOM is calculated on this mission with a conventional ATR 42-500 like aircraft model implemented in SUAVE. All conventional aircraft fly this mission at an altitude of 21 000 ft, while the hybrid electric aircraft is designed to fly at altitude of just 17 000 ft, optimized for NOx impact. This flight level reduction leads to a NOx FOM improvement of 81 %, while improving the CO2 emissions by 14 % compared to the ATR 42-500 [1]. In total, the ATR 42-500 like aircraft has a fuel burn of 1341 kg including reserves and 548 kg for the trip alone. The mission profile including reserves is shown in Figure 5. The mission consists of the main mission, including climb, cruise and descent, and the reserves. The reserves include a diversion mission and a 45 min extended cruise (holding).

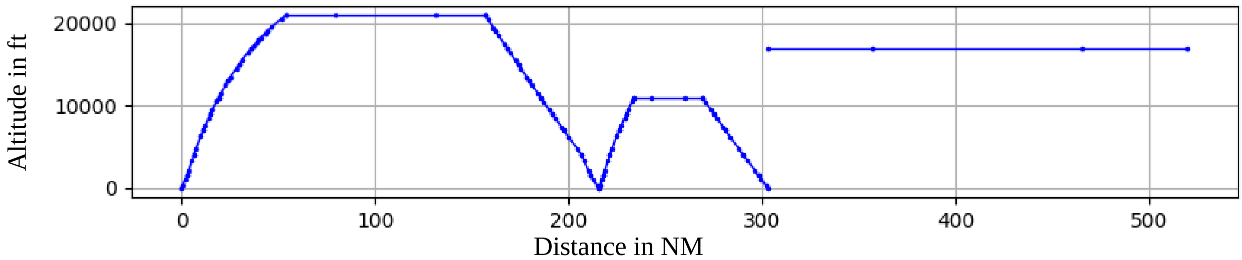

Figure 5: Evaluation mission for the regional aircraft comparison

4. Design case study on payload range capabilities

Since for both cryogenic aircraft the fuel tank volume is a sizing parameter, several design strategies can be followed for these aircraft. The first approach would be to choose the same design point as for conventional aircraft. This results in an aircraft with a rather small fuel tank and hence low operational flexibility, since the fuel tank is sized for the design mission only. For conventional aircraft, the fuel volume in the wing is usually bigger than the fuel volume used for the design mission. Therefore, with ranges larger than the design point range for cryogenic propulsion architectures, the borderline in the payload range diagram kinks and drops sharply, as shown in Figure 6. In addition, the maximum take-off mass (MTOM) line of the payload-range diagram becomes shallower for fuels with higher gravimetric energy densities, implying a more fuel-efficient aircraft. This means that an aircraft with a shallower MTOM-line can cover a larger distance with 1 kg of fuel than an aircraft with a steeper MTOM line. The results shown in Figure 6 reflect these considerations.

Because of the different gravimetric energy densities of the three fuels, a prediction on the aircraft efficiency solely based on the payload range diagram is not possible. For the HRA, the shallower slope of the MTOM line results in a reduced maximum payload of 5700 kg instead of the anticipated 5800 kg required in the FUTPRINT50 TLARS [31].

DOI: 10.13009/EUCASS2023-904

The MRA on the other hand has a reduced range with maximum payload, nevertheless fulfilling the payload requirements stated in the TLARs. Following this strategy results in a similar ferry range for both cryogenic aircraft of approximately 1000 NM.

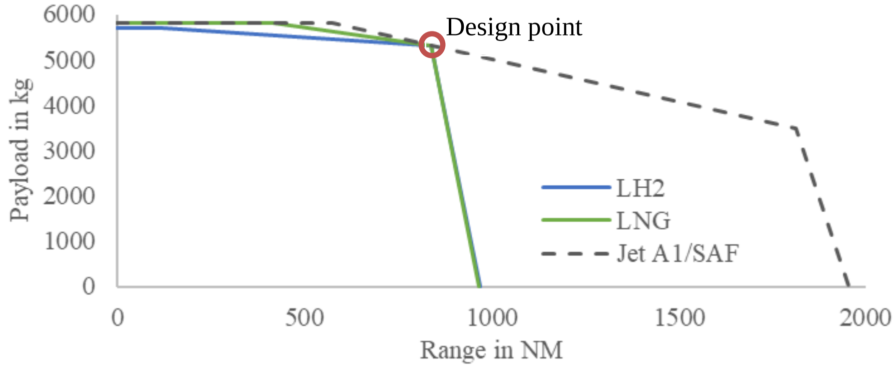

Figure 6: Payload-range diagrams for identical design points of MRA, HRA and CRA 2040

A second strategy to configure a more flexible aircraft would be to design for two points simultaneously: the range at maximum payload and the ferry range, see Figure 7. The fuselage of the aircraft in this case is still sized for 50 passengers, however, it has a reduced design payload mass and an increased design range. For the MRA, the design point in this case is at 1770 NM with 4350 kg payload. The HRA design point is at 1750 NM with 5050 kg payload. The resulting range with the maximum payload of 5800 kg following this strategy is between 530 NM and 578 NM for all three aircraft.

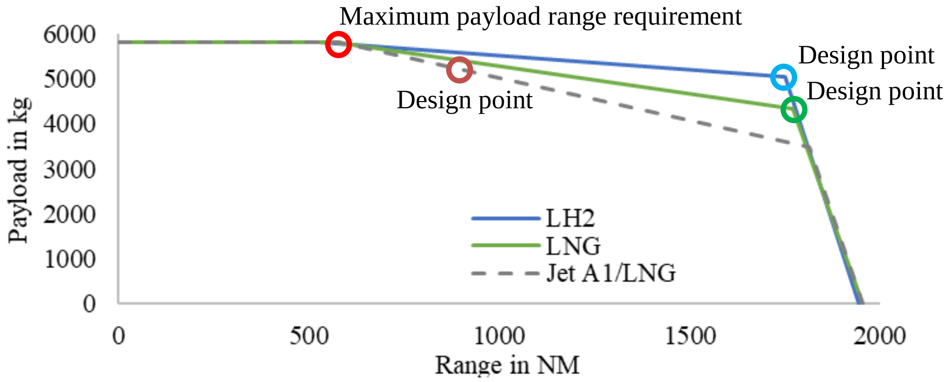

Figure 7: Payload-range diagrams for identical maximum payload range of MRA, HRA and CRA 2040

This design strategy results in highly flexible cryogenic aircraft. However, the resulting fuel tank mass reduces the performance of the aircraft. Hence, a third strategy is investigated, compare Figure 8. By reducing the range at maximum payload, while keeping the ferry range similar to the conventional aircraft, the design payloads can be further reduced. In this case, the only requirements would be, to have the conventional design point within the operational capabilities of all ICE aircraft, and that all aircraft are capable of flying with the maximum payload. This results in lower OEM for the cryogenic aircraft compared to the second strategy, ultimately resulting in a better performance.

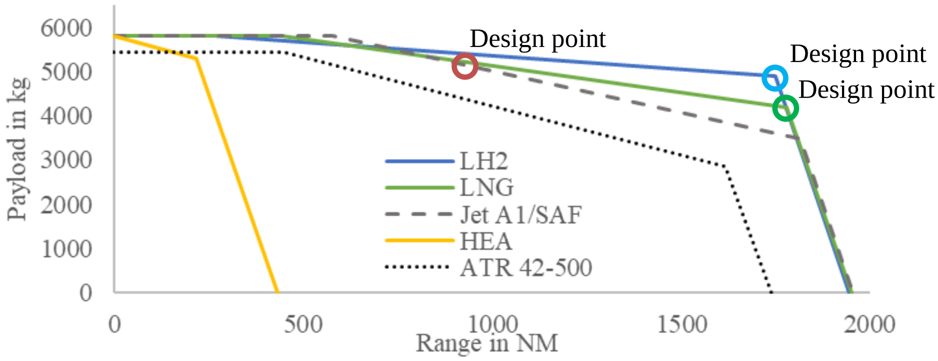

Figure 8: Payload-range diagrams for identical ferry ranges of the ICE aircraft including ATR 42-500 and HRA with design points at 840 NM with 4560 kg payload and 216 NM with 5300 kg payload

DOI: 10.13009/EUCASS2023-904

5. Environmental and economical assessment

In this section, the performance of the HRA and MRA are compared based on the design strategies described in Section 4. The performance comparison is based on the FOM as described above. The FOM for each aircraft is calculated for low cost and high net carbon intensity fuels as well as for high fuel price and low net zero carbon intensity. The values calculated for this study are based on the fuel price data given in Table 2 and, given the fluctuations in fuel prices, may vary for different assumption and future scenarios. The prices can easily be adapted as described in Section 3.1. In a first step, only the total FOM, the environmental FOM and the single FOM (sFOM) for cash operating costs (COC) and CO2 are assessed. These are the sFOM that are impacted the most by varying fuel prices and carbon intensity. In Figure 9, the FOM for the MRA are plotted for the three different design points as described in Section 4. The first diagram on the right shows the values for the conventional design point at 840 NM with 5300 kg. With the assumption that carbon neutral fuel is the most expensive, the COC FOM decreases with increasing fuel prices, while the FOM related to CO2 increases. The highest total FOM in this case is reached for the lowest fuel price. However, the FOM for fossil LNG is only 1.6 % higher than that for renewable LNG, despite a significantly lower COC FOM. In the first scenario, none of the considered FOM falls below that of the ATR 42-500, which is calibrated to 0 for the use with Jet A-1. The second plot shows a similar behaviour, with a more significant decrease in the COC FOM. The total FOM following this strategy is 4.3 % lower than for the conventional design point layout. The decrease can be related to an oversized and heavy fuel tank, making the aircraft less efficient. Reducing the maximum range with maximum payload helps improving the minimum COC FOM by 1.7 % to -0.0056 compared to the previous approach. The total FOM can thereby be increased by 1.1 %. The highest total FOM of 0.2894 is reached for the first design strategy. The third strategy results in a maximum FOM of 0.2802. With 0.2771, the second strategy produces the lowest performing aircraft.

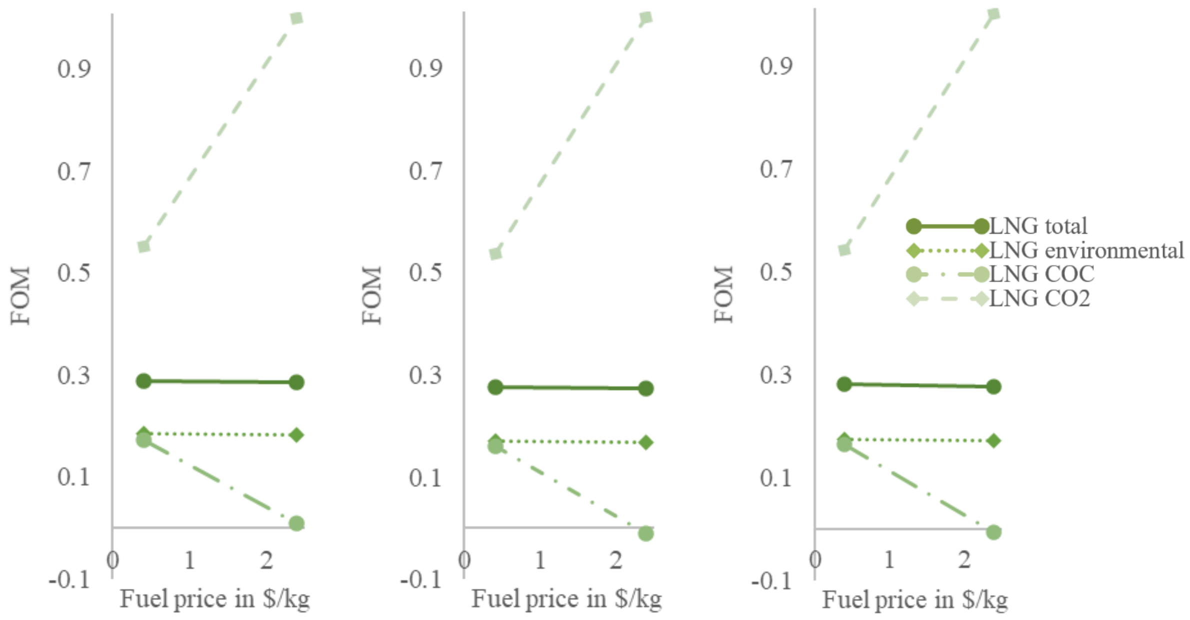

Figure 9: FOM of the MRA depending on fuel price and CO2 intensity for every design strategy, with a reference FOM of 0 from the ATR

For the evaluation criteria chosen in this study, the MRA produces the best FOM when fossil LNG is used. This may change with varying fuel cost for both fossil and renewable LNG or by adapting the assessment criteria.

In contrast to this, the FOM plotted in Figure 10, showing the values for the HRA, imply a different trend for hydrogen. For all three design methods, green hydrogen shows the best performance regarding total FOM as well as environmental FOM. Also, the differences in the maximum and minimum FOM are more significant for hydrogen, with changes of up to 41 % in the total FOM. Similar to the results of the MRA, the HRA has the highest total FOM when choosing the conventional design point of 840 NM with 5300 kg payload. In this design case a maximum FOM of 0.3211 is achieved. Again, the third design method provides the second highest FOM of 0.2889. Strategies two and three result in low COC FOM for green LH2. These values are between 5 % and 5.5 % lower than the reference set by the ATR 42-500.

DOI: 10.13009/EUCASS2023-904

If the decision for the best design point for cryogenic aircraft would only be based on the highest FOM, a conventional design point would be the apparent solution. However, as described in Section 4, the flexibility and, in case of the MRA, also the maximum payload capabilities are thereby reduced. The approach delivering the highest FOM and also acceptable payload-range flexibility would be the third presented in Section 4. Both the MRA and the HRA show similar maximum FOM for this method. The final comparison to the CRA 2040 and HRA is performed against these versions of the MRA and HRA.

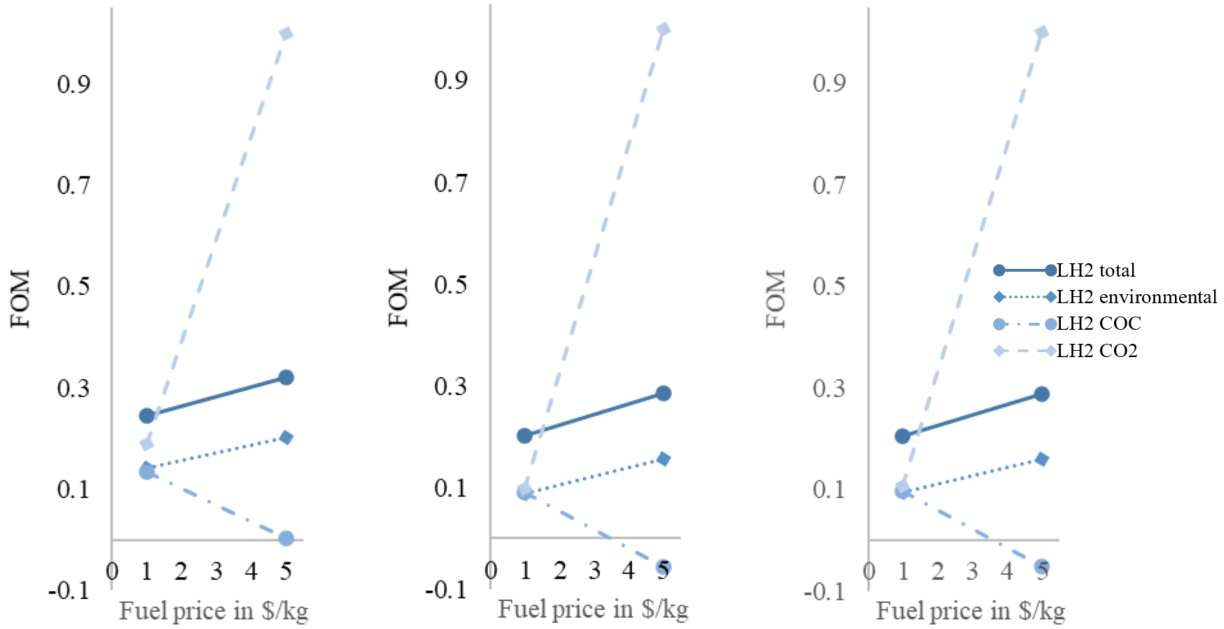

Figure 10: FOM of the HRA depending on fuel price and CO2 intensity for every design strategy, with a reference FOM of 0 from the ATR

To provide consistent results, the FOM of the CRA 2040 are also calculated for different carbon intensities linked to increasing fuel prices. The conventional aircraft is obviously only designed for the conventional design point. The resulting changes in the FOM are plotted in Figure 11.

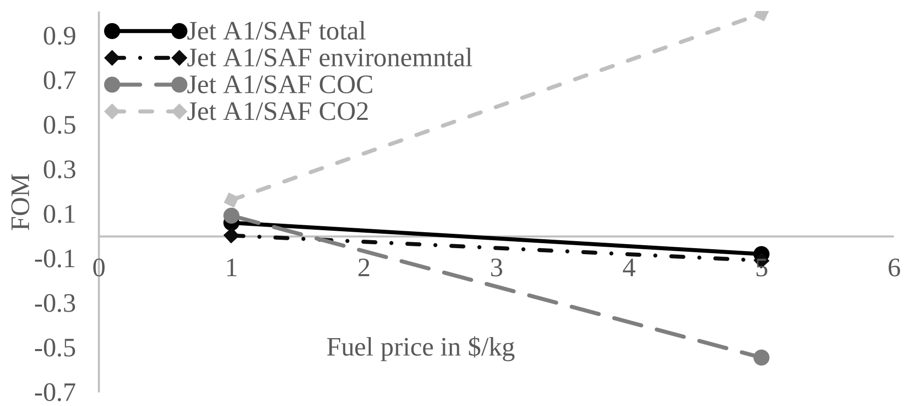

Figure 11: FOM of the CRA 2040 depending on fuel price and CO2 intensity, with a reference FOM of 0 from the ATR

All FOM of the conventional aircraft except CO2 show a downward trend. The total FOM decreases below ATR level for a blending ratio SAF/Jet A-1 of more than 50 %. The highest total FOM of 0.05 is similar to the LNG aircraft for 100 % fossil fuel. A CRA 2040 flying with 100 % carbon neutral SAF, would have a total FOM of -0.0791.

DOI: 10.13009/EUCASS2023-904

6. Results and outlook

In this section the resulting aircraft designs from Section 5 are described and evaluated. The mass breakdown for all six aircraft on each corresponding design mission, is given in Figure 12. Since all aircraft have a different design point, different payload masses result.

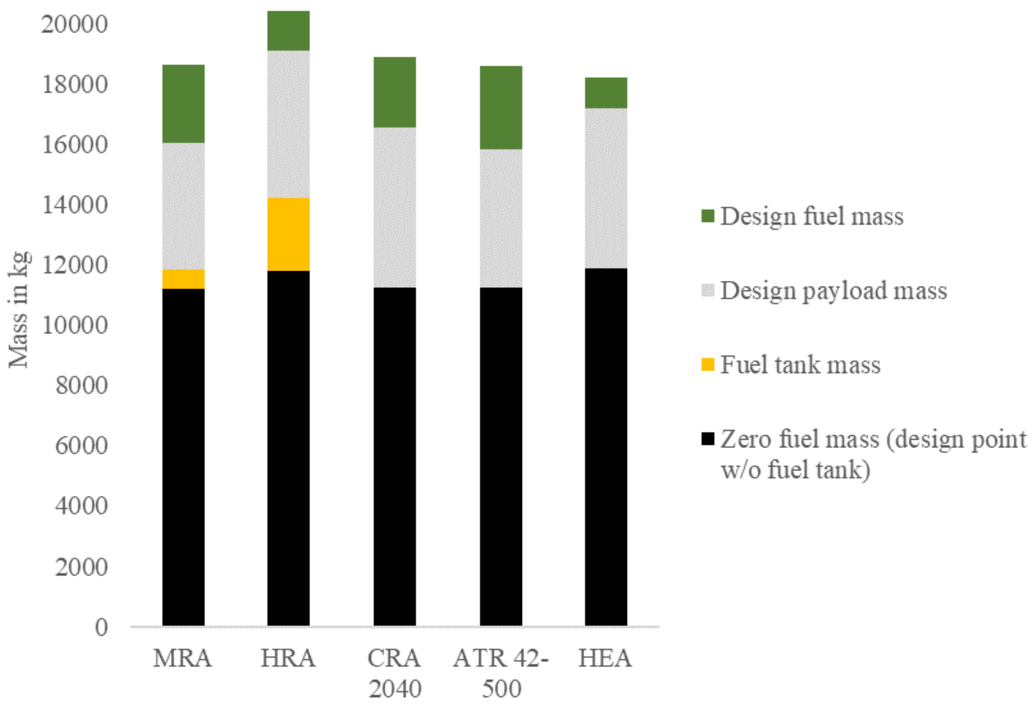

Figure 12: Mass breakdown comparison of the MRA, HRA CRA 2040, ATR 42-500 and HEA

The HRA has the highest zero fuel mass (ZFM) and also MTOM in the design point, which is a result of the heavy fuel tank. The combined fuel tank and fuel mass are similar for the MRA and the HRA, the resulting system specific gravimetric index was already described in [24].

On the evaluation mission of 400 km with 5300 kg payload, the following optimum total FOM result for each aircraft with the ATR 42-500 using fossil Jet A-1 as the baseline:

- ATR 42-500: 0.00 Jet A-1, no SAF
- CRA 2040: 0.05 Jet A-1, no SAF
- HEA: 0.19 Jet A-1, no SAF
- MRA 0.28 fossil LNG
- HRA 0.29 green LH2

These results are based on the evaluation methods available in the FUTPRINT50 SUAVE structure and may vary with higher fidelity methods. Such investigations should be part of future research. This study concludes that according to the FOM, a SAF-fueled aircraft would be the worst option. Furthermore, SAF is more expensive than fossil LNG and grey LH2, which are quite similar in price. Looking at the renewable options, the same trends can be seen. This study has shown that SAF is 16 times more expensive than fossil LNG or 14 times than fossil LH2 for the same amount of energy available. These price differences lead to SAF fueled aircraft beeing the worst option according to the FOM. The LNG and LH2 counterparts perform almost equally and are not directly distinguishable. Thus, a selection should be made solely on the availability of the fuel and implications on infrastructure development and related costs. Furthermore, if same operational flexibility should be achieved, a new design point needs to be chosen. In comparison to conventional aircraft, where the tank is not completely filled in the design point, for the LNG and LH2 designs, the tank would be full in the design point.

DOI: 10.13009/EUCASS2023-904

Acknowledgments

The research leading to these results has received funding from the European Union's Horizon 2020 Research and Innovation program under Grant Agreement No. 875551.

References

[1] F. Brenner, D. Eisenhut , J. Mangold and N. Moebs, "Deliverable 4.3 Evaluation against reference aircraft," FutPrInt50, Stuttgart, 2023.

[2] J. Mangold, d. Silberhorn, N. Moebs, N. Dzikus, J. Hoelzen, T. Zill and A. Strohmayer, "Refueling of LH2 Aircraft—Assessment of Turnaround Procedures and Aircraft Design Implication," *Energies,* p. https://doi.org/10.3390/en15072475 , 2022.

[3] F. Brenner, "Preliminary Design of a Sustainable Long-Range Aircraft," Masters Thesis, University of Stuttgart, Stuttgart, 2021.

[4] J. Mangold, "Economical assessment of hydrogen short-range aircraft with the focus on the turnaround procedure," Master's Thesis, Unicersity of Stuttgart, Stuttgart, 2021.

[5] C. Hebling, M. Ragwitz, T. Fleiter, U. Groos, D. Härle, A. Held, Jahn, N. Müller, T. Pfeifer, P. Plötz, O. Ranzmeyer, A. Schaadt, F. Sensfuß, T. Smolinka and M. Wietschel, "Eine Wasserstoff-Roadmap für Deutschland," Frauenhofer, Karlsruhe and Freiburg, 2019.

[6] Fuel Cells and Hydrogen 2 Joint Undertaking, "Hydrogen-powered aviation : a fact-based study of hydrogen technology, economics, and climate impact by 2050," Publications Office, https://data.europa.eu/doi/10.2843/471510, 2020.

[7] A. Cobanoglu, "Environmental and Economic Evaluation of Retrofit LNG-Powered Transport Aircraft," Master's Thesis University of Stuttgart, Stuttgart, 2023.

[8] D. Silberhorn, J. Hartmann, N. Dzikus, G. Atanasov, T. Zill, J. C. Gomez Trillos, M. Oswald, U. Brand, T. Vogt and W. Grimme, "The Air-Vehicle as a Complex System of Air Transport Energy Systems," AIAA, 10.2514/6.2020-2622, 2020.

[9] K. Steeckt, "Conceptual design and investigation of hydrogen-fueled regional freighter aircraft," KTH, School of Engineering Sciences (SCI), Aeronautical and Vehicle Engineering, URN: urn:nbn:se:kth:diva-26348, 2010.

[10] IATA, "Jet Fuel Price Monitor," [Online]. Available: https://www.iata.org/en/publications/economics/fuel-monitor/. [Accessed 05 07 2023].

[11] D. Gerstein and A. Bollien, "Fact Sheet BioLNG," DVGW, https://www.dena.de/fileadmin/dena/Dokumente/Pdf/LNG_Taskforce/20211018_FactSheet_BioLNG_2021.pdf, 2021.

[12] J. Hoelzen, Y. Liu, B. Bensmann, C. Winnefeld, A. Elham, J. Friedrichs and R. Hanke-Rauschenbach, "Conceptual Design of Operation Strategies for Hybrid Electric Aircraft," Energies, https://doi.org/10.3390/en11010217 , 2018.

[13] M. Klöwer, M. Allen, D. Lee, S. Proud, L. Gallagher and L. Skowron, "Quantifying aviation's contribution to global warming," IOP Science, DOI:10.1088/1748-9326/ac286e, 2021.

[14] M. Yahyaoui, A. Anantha-Subramanian and Lombaert-Valot, "The Use of LNG as Aviation Fuel: Combustion and Emissions," in *AIAA Propulsion and Energy Forum and Exposition 2015At: Orlando-Florida*, DOI: 10.2514/6.2015-3730, 2015.

[15] R. Carter, "Development Of A Liquid Hydrogen Combustion High Bypass Turbofan Model In NPSS," Washington University in St. Louis, https://openscholarship.wustl.edu/cgi/viewcontent.cgi?article=1163&context=mems500, 2021.

[16] IATA, "Developing Sustainable Aviation Fuel (SAF)," [Online]. Available: https://www.iata.org/en/programs/environment/sustainable-aviation-fuels/. [Accessed 05 07 2023].

[17] W. Affonso, Jr., et al., "System architectures for thermal management of hybrid-electric aircraft - FutPrInt50," IOP Conf. Ser.: Mater. Sci. Eng., 2022.

[18] J. Mangold, D. Eisenhut, F. Brenner, N. Moebs and A. Strohmayer, "Preliminary hybrid-electric aircraft design with advancements on the open-source tool SUAVE," Conference: 12th EASN International

DOI: 10.13009/EUCASS2023-904

Conference on "Innovation in Aviation & Space for opening New Horizons"At: Barcelona, Spain, DOI: 10.1088/1742-6596/2526/1/012022, 2023.

[19] E. Botero, A. Wendorff, T. MacDonald, A. Variyar, J. Vegh, T. Lukaczyk, J. Alonso, T. Orra and C. Ilario da Silva, "SUAVE: An Open-Source Environment for Conceptual Vehicle Design and Optimization," in *AIAA 2016-1275 Session: Aircraft Design Tools*, https://doi.org/10.2514/6.2016-1275, 2016.

[20] FutPrInt50, "SUAVE FutPrInt50," [Online]. Available: https://github.com/FutPrInt50/SUAVE. [Accessed 05 07 2023].

[21] F. Brenner, J. Mangold, D. Eisenhut, N. Moebs and A. Strohmayer, "Deriving a year 2040 reference aircraft from a modern turboprop, implemented and calibrated in SUAVE," in *Conference: 12th EASN International Conference on "Innovation in Aviation & Space for opening New Horizons"At: Barcelona, Spain*, DOI: 10.1088/1742-6596/2526/1/012009, 2023.

[22] D. Eisenhut, J. Mangold, N. Moebs, F. Brenner and A. Strohmayer, "Case study on hybrid-electric aircraft designs enabled by an enhanced SUAVE version," in *Conference: 12th EASN International Conference on "Innovation in Aviation & Space for opening New Horizons"At: Barcelona, Spain*, DOI: 10.1088/1742-6596/2526/1/012019, 2023.

[23] D. Brewer, Hydrogen Aircraft Technology, CRC Press, 1991.

[24] J. Mangold, F. Brenner, N. Moebs and A. Strohmayer, "Aircraft Design Implications of Alternative Fuels for Future Hybrid-Electric Regional Aircraft Configurations," in *Conference: EUCASS-3AF 2022 - 9th European Conference for Aerospace SciencesAt: Lille, France*, DOI: 10.13009/EUCASS2022-7294, 2022.

[25] U. Schumann, "Aircraft Emissions," Encyclopedia of Global Environmental Change, ISBN 0-471-97796-9, 2002.

[26] F. Svensson, "Potential of reducng the environmental impact of civil subsonic aviation by using liquid hydrogen," Cranfield CERES, http://dspace.lib.cranfield.ac.uk/handle/1826/10726 , 2005.

[27] J. Thorbeck, "DOC-Assessment Method," TU Berlin, https://www.fzt.haw-hamburg.de/pers/Scholz/Aero/TU-Berlin_DOC-Method_with_remarks_13-09-19.pdf, 2013.

[28] European Commission, "Flightpath 2050," European Commission, European Union, 2011.

[29] E. COMMISSION, "The European Green Deal," EUROPEAN COMMISSION, European Union, 2019.

[30] R. Reis, F. Odaguil, E. Windels, Y. Teeuwen, J. van der Pols, P. Laskaridis, D. Bergmann, D. Eisenhut, N. Moebs and F. Brenner, "Deliverable 2.1 Requirements and Reference Aircraft," FutPrInt50, 2022.

[31] D. Eisenhut, N. Moebs, E. Windels, D. Bergmann, I. Geiß, R. Reis and A. Strohmayer, "Aircraft Requirements for Sustainable Regional Aviation," aerospace, https://doi.org/10.3390/aerospace8030061, 2020.